Metal-insulator transition in $La_{1.85}Sr_{0.15}CuO_4$ with various substitutions for Cu

Marta Z. Cieplak,* S. Guha, H. Kojima, and P. Lindenfeld
Department of Physics, Rutgers University, Piscataway, New Jersey 08855

Gang Xiao
Physics Department, Brown University, Providence, Rhode Island 02912

J. Q. Xiao and C. L. Chien
Department of Physics and Astronomy, The Johns Hopkins University, Baltimore, Maryland 21218
(Received 18 February 1992; revised manuscript received 6 May 1992)

We have measured the resistance and magnetoresistance of $La_{1.85}Sr_{0.15}CuO_4$ with five different impurities (Zn, Ni, Ga, Co, and Fe) substituted for Cu, down to 50 mK, and in magnetic fields up to 8 T. The concentration x_c at which superconductivity disappears is smaller than the concentration x_{MI} at which the metal-insulator (MI) transition occurs, leaving in each case a metallic, nonsuperconducting region of concentration. We show that x_{MI} is determined by a superposition of the impurity-induced disorder and the carrier concentration. x_c, on the other hand, is a function of the effective local magnetic moment induced by the impurity. In the metallic specimens σ varies with $\sqrt{T}$ up to a temperature T^* which increases with the effective local magnetic moment induced by the impurity, and for Fe reaches 70 K. The magnetoresistance is negative except in the presence of superconducting fluctuations. We conclude that these features are the result of the influence of spin scattering on the electron-electron interactions. In strongly insulating specimens the resistivity varies as $\rho = \rho_0 \exp(T_0/T)^{1/2}$. We demonstrate that the behavior is consistent with variable-range hopping in the presence of a Coulomb gap, and describe the conditions under which the exponent may change to 1/4 in the vicinity of the MI transition.

I. INTRODUCTION

In spite of the theoretical and experimental interest in the metal-insulator (MI) transition there are surprisingly few systems for which it has been studied in detail. The reason is, in part, that it is necessary to go to low temperatures, usually well below 1 K, to determine the value of the zero-temperature electrical conductivity, so as to determine the metallic or insulating character of a particular specimen. The determination is often complicated by the intervention of superconductivity. At the same time the relation of the disappearance of superconductivity to the presence of the MI transition is an additional subject of special importance, where we have, so far, only fragmentary evidence about the controlling parameters.

In this paper we describe the MI transition in $La_{1.85}Sr_{0.15}CuO_4$ produced by the addition of five different impurities substituted for Cu. We examine the influence of the change in the carrier concentration, of the disorder-induced electron localization, and of the magnetic scattering. In addition to the effect of these factors on the MI transition we seek to determine their relation to the disappearance of superconductivity.

In $La_{1.85}Sr_{0.15}CuO_4$ all copper atoms are in copper-oxide planes and the impurities are known to substitute at the Cu sites.[1–8] This relative simplicity of the structure of the "2-1-4" system makes it a model system for studying the effect of impurities and, in particular, of their magnetic moments, on high-T_c superconductivity.

One of the most intriguing effects of the substitutions is that both magnetic and nonmagnetic impurities induce local magnetic moments in the CuO_2 planes.[9,10] This is because nonmagnetic impurities, such as Zn or Ga, remove copper spins and so create spin vacancies.

Relatively small amounts of the impurities have a drastic effect on the properties as they bring the material rapidly to the MI transition and cause superconductivity to be suppressed.[1–7,9] We show that the value of the impurity concentration, x_{MI}, at which the MI transition takes place is larger than the value x_c where superconductivity disappears, for all five impurities that we have studied, so that there is in each case a metallic nonsuperconducting phase adjacent to the MI transition. We also demonstrate that the value of x_{MI} is determined by two factors, namely the change in carrier concentration and the impurity-induced disorder, while x_c correlates with the magnitude of the local magnetic moment. The detailed examination of the change of conductivity, σ, with temperature and magnetic field shows that the spin scattering affects the quantum corrections to the conductivity at low temperatures. This indicates the importance of spin scattering, and confirms the conclusion that this factor (rather than localization) is responsible for the de-

struction of superconductivity.[9] We have also determined that the value of the critical exponent with which the normal-state conductivity goes to zero at x_{MI} is equal to 0.92 ± 0.1 for Fe and 0.7 ± 0.1 for Zn impurities.

In addition the detailed examination of $\sigma(T)$ on the insulating side of the MI transition leads to a better understanding of the changes in the functional dependence of this quantity as the MI transition is approached. Specifically we show under what conditions a change in the exponential dependence of the resistivity, $\rho = \rho_0 \exp (T_0/T)^{\mu}$ from a value of the exponent μ of 1/2 to the value 1/4 may be expected.

II. EXPERIMENT

A. Sample preparation

We have made five series of polycrystalline samples of the type $La_{1.85}Sr_{0.15}Cu_{1-x}A_xO_4$, with A one of Fe, Co, Ni, Zn, or Ga, by the solid-state reaction method,[7] with concentrations x up to 6 at.% for Co, Ni, and Ga, up to 10 at.% for Fe, and up to 20 at.% for Zn.

The samples are consistent and reproducible, and x-ray-diffraction analysis does not show any signs of other phases. We have not measured the oxygen content, but it has been shown that Zn can be substituted without any change in the oxygen content,[5] and there are strong indications that this is the case for the other impurities also. Hall-effect data for our samples[11] indicate a reduction of the carrier concentration which is consistent with the valence of the impurities rather than with a change of oxygen content. Some of these samples have also been used in studies of the susceptibility[9] and of electron spin resonance.[12]

B. Conductivity measurements

The samples are between 1 and 2 cm long, with a cross-sectional area of the order of several mm^2. Four indium strips are cold pressed to each sample for four-terminal resistance measurements.

The resistance of most of the samples was measured from 3 K to room temperature in a conventional cryostat, and from 50 mK to 1 K in a dilution refrigerator. Some of the samples were also measured in magnetic fields up to 8 T.

Many precautions were taken to ensure the reliability of the measurements in the dilution refrigerator. I-V measurements were made at each temperature so as to check for heating and other sources of nonlinearity. An extensive series of tests showed that the temperature measurements were reliable down to 50 mK.

III. EXPERIMENTAL RESULTS

Figures 1 and 2 show the normalized resistivity $\rho(T)/\rho(297)$ as a function of temperature from room temperature (297 K) to 3 K for the specimens substituted with Fe and Co. These figures are qualitatively similar to those with Ga, Zn, and Ni impurities.[7,13] They illustrate the decrease in the superconducting transition temperature T_c with impurity concentration x, and the accompanying change in the character of the normal-state electrical transport as the linear $\rho(T)$ in the pure parent material gives way to the upturn at low T which is characteristic of electron localization.

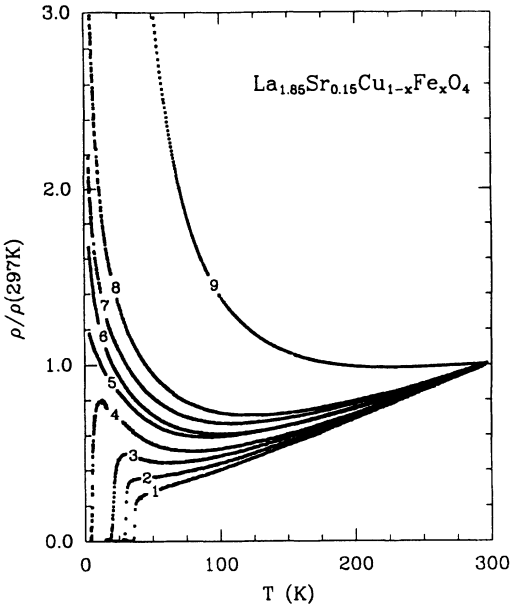

FIG. 1. The temperature dependence of the normalized resistivity for samples with various amounts of Fe (in at.%): 1–0%, 2–0.4%, 3–0.8%, 4–1.5%, 5–1.8%, 6–2.4%, 7–3%, 8–4%, 9–10%.

Figure 3 shows the dependence of $\rho(297\,\mathrm{K})$ on x, indicating a linear change up to about 4 at.% for all impuri-

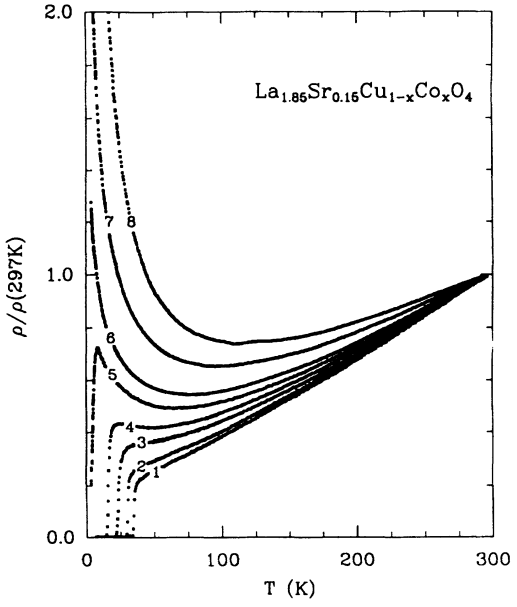

FIG. 2. The temperature dependence of the normalized resistivity for samples with various amounts of Co (in at.%): 1–0%, 2–0.4%, 3–0.8%, 4–1.5%, 5–1.8%, 6–2.4%, 7–3%, 8–6%.

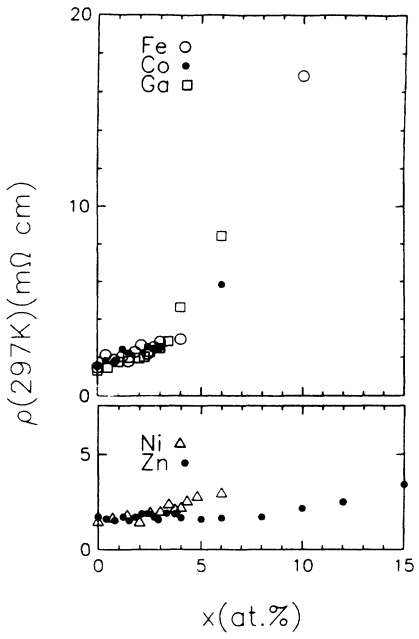

FIG. 3. The room-temperature resistivity, $\rho(297\ \mathrm{K})$, as a function of the impurity concentration x for the five impurities.

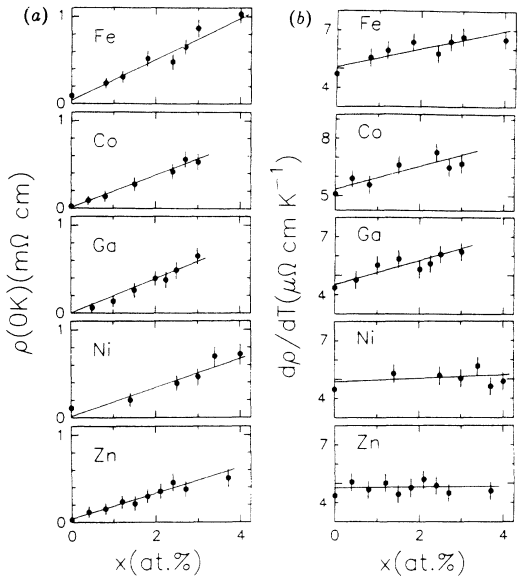

FIG. 4. Between 200 and 300 K the resistivity varies linearly with T, $\rho = \rho_0 + (d\rho/dT)T$. (a) ρ_0 vs x and (b) $d\rho/dT$ vs x for the five impurities.

ties, followed by a dramatic increase for Fe, Co, and Ga. This difference in the ρ dependence of x correlates with the nominal valence of the impurity, 3+ for Fe, Co, and Ga impurities, and 2+ for Zn and Ni. The trivalent impurities reduce the number of the free carriers (holes) and so affect the resistivity more strongly than the divalent impurities.

For all samples with small impurity contents, $x < 4$ at.%, the high-temperature resistivity data in the region 200–300 K may be fitted with the linear function $\rho = \rho(0\,\mathrm{K}) + (d\rho/dT)T$. The dependence of $\rho(0\,\mathrm{K})$ and $d\rho/dT$ on x is shown in Fig. 4. It is seen that $\rho(0\,\mathrm{K})$ increases linearly with the impurity content for all of the impurities. The slope, however, increases linearly with x only for the trivalent impurities, and is approximately constant for the divalent ones.

In Fig. 5 we show the behavior down to 50 mK for a series of 14 representative specimens, illustrating the progression from superconducting to insulating behavior. The arrow indicates the resistivity ρ_M corresponding to the estimate of the Mott minimum metallic conductivity where the MI transition may be expected. If we assume that superconductivity in our specimens is largely two-dimensional we can use $\sigma_M^{2D} \sim 0.1e^2/\hbar = 3.9\times10^{-5}\ \Omega^{-1}$. For a random mixture of 2D crystallites we then have $\sigma^{3D} = \sigma^{2D}/2d$, where we use for d the distance between CuO_2 planes, so that $\rho_M = (\sigma_m^{3D})^{-1} = 3.3\times10^{-3}\ \Omega\,\mathrm{cm}$.

We may divide the specimens into three groups. Specimens 1–4 follow the relation $\rho = \rho_0 \exp(T_0/T)^{1/2}$ at low temperatures and are clearly insulating.

For the next group of specimens (5–9) the T dependence of ρ becomes slower below 1 K. We replot the data on Figs. 6(a) and 6(b) against $T^{-1/4}$. The relation $\rho = \rho_0 \exp(T_0/T)^{1/4}$ has been widely quoted as being observed in insulating specimens. We see that it is followed in specimens 5 and 6 below 1 K and perhaps in specimens 7, 8, and 9 for an even more limited temperature range. We will assume that ρ continues to increase as T decreases toward zero, so that these specimens are on the insulating side of the MI transition.

Finally, specimens 10–15 exhibit a normal-state conductivity which is different from zero as T goes to zero

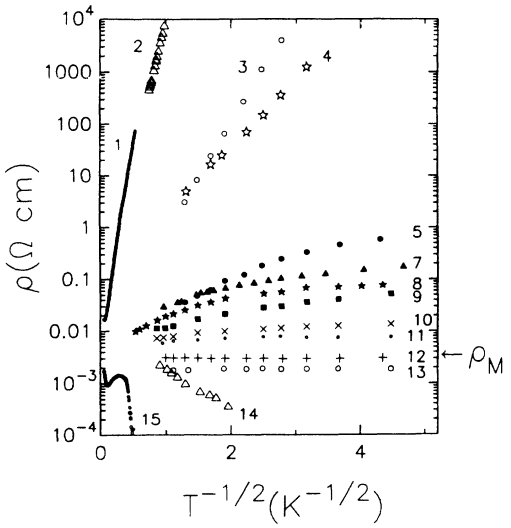

FIG. 5. The resistivity as a function of $T^{-1/2}$ for a series of specimens (in at.%): 1—Fe 10%, 2—Ga 10%, 3—Zn 20%, 4—Co 6%, 5—Zn 12%, 7—Ga 4%, 8—Fe 4%, 9—Ga 3.4%, 10—Fe 3%, 11—Fe 2.7%, 12—Co 3%, 13—Zn 3.7%, 14—Ga 2.5%, 15—Fe 1.5%. (The curve for sample 6, Ni 6%, is close to that of sample 5 and is not shown.)

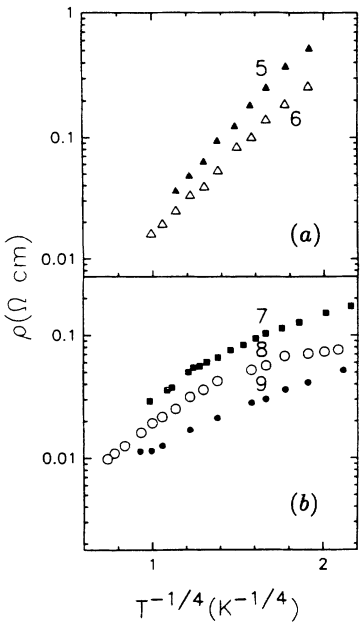

FIG. 6. The resistivity as a function of $T^{-1/4}$ for several specimens close to the MI transition (in at.%). (a): 5—Zn 12%, 6—Ni 6%; (b): 7—Ga 4%, 8—Fe 4%, and 9—Ga 3.4%.

so that they are metallic. In Figs. 7(a)–7(e) we plot σ against $\sqrt{T}$. We see that the relation $\sigma = \sigma_0 + m\sqrt{T}$ is followed at low T for the specimens which are metallic but not superconducting. The upturn at the lowest T for the higher values of σ_0 indicates superconducting fluctuations. We have shown that they can be suppressed by a magnetic field.

It may be seen that the temperature range for which the $\sqrt{T}$ dependence is followed varies with the type of impurity. It is small (up to 1.5 K) for Zn and Ni, somewhat larger (up to about 2.2 K) for Ga and Co, and unexpectedly large (up to about 70 K) for Fe. The slope m varies with the type of impurity and also with the impurity concentration.

Figures 8(a)–8(d) show $\rho(H)/\rho(0)$ against magnetic field H for several specimens with Fe, Ni, Zn, and Ga impurities. We see that the magnetoresistance is positive for the lower concentrations, indicative of the gradual suppression of superconducting fluctuations by the magnetic field. For higher values of x, when superconducting fluctuations are small or absent, the magnetoresistance is negative.

In order to gain more precise information about the value x_{MI} of the concentration at which the MI transition takes place, we have extrapolated the normal-state conductivity to the value σ_{00} at $H = 0$ and $T = 0$ for each metallic specimen. In Fig. 9 we show the values of σ_{00} as a function of x. For the samples with zinc and iron impurity there are sufficient data to attempt to determine the functional dependence of σ_{00} on x. As shown in Fig. 9 the Fe data are consistent with a linear fit, while a nonlinear fit is better for the Zn data. We return to this question later in the section on the critical exponent.

For both these impurities the concentration x_{MI} at the MI transition is considerably larger than the value x_c where T_c goes to zero. This is also the case for the re-

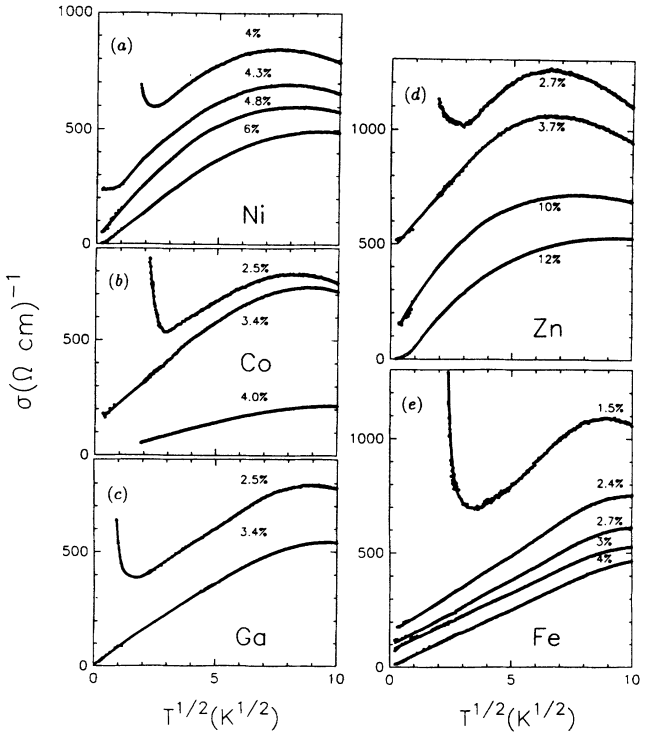

FIG. 7. The conductivity vs $\sqrt{T}$ for five series of samples each with a different impurity: (a) Ni, (b) Co, (c) Ga, (d) Zn, and (e) Fe.

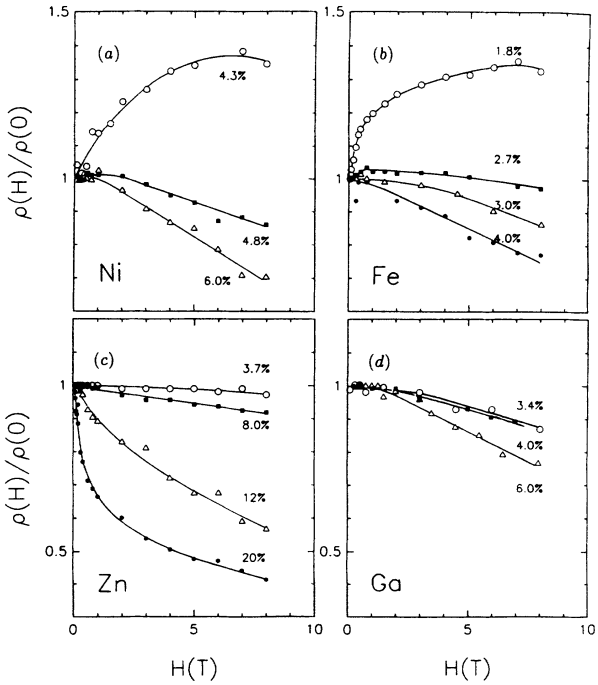

FIG. 8. The magnetoresistance $\rho(H)/\rho(0)$ at 100 mK as a function of the magnetic field for samples with various impurities: (a) Ni, (b) Fe, (c) Zn, and (d) Ga.

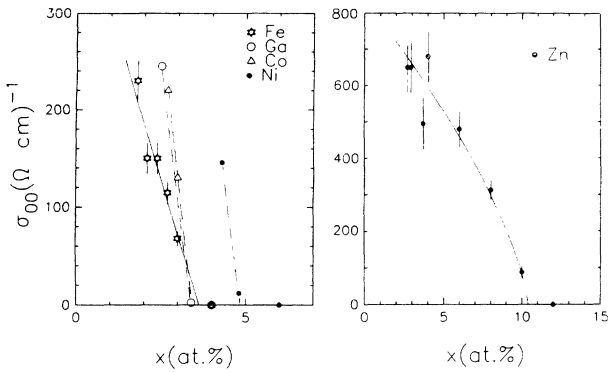

FIG. 9. σ_{00}, the normal-state conductivity extrapolated to $T = 0$ and $H = 0$, as a function of x for the five different impurities. The points for the Zn system with $x = 2.7, 2.9, 4$, and 6 at.% have been obtained without the application of the magnetic field, i.e., by the extrapolation of the high-temperature values of conductivity vs $\sqrt{T}$ to $T = 0$.

maining impurities, Co, Ni, and Ga, for which we obtain an approximate value for x_{MI} by assuming a linear dependence of σ_{00} on x. In each case, therefore, there is a range of concentrations for which the specimens are metallic but not superconducting (see Table I).

IV. DISCUSSION

A. Metallic side of the MI transition

1. *What drives the metal-insulator transition?*

In this section we discuss the changes in the metallic specimens, brought about by the addition of impurities, which cause the material to lose its metallic character, and eventually to become an insulator at the concentration x_{MI}.

The most obvious effect on the MI transition is that of the charge-carrier concentration n. Our knowledge about n comes from measurements of the Hall effect.[11] The interpretation of Hall-effect measurements in the perovskites is beset by a number of obscure factors, chief among which is the strong temperature dependence of the Hall coefficient R_H. Until this feature is understood and related questions are resolved, deductions made from the Hall effect must be viewed with caution. With this proviso we proceed nevertheless to extract information from the Hall-effect data about the changes in carrier concentration, Δn, with changes in x.

We gain confidence from the decrease in the temperature dependence of R_H as T decreases, and use the values of R_H at 80 K, where the T dependence is quite weak. The changes $\Delta n/n$ per percent of impurity, are listed in Table I. We note that Δn correlates at least partly with the nominal valence of the added impurities. The trivalent impurities Fe, Co, and Ga have similar effects as they add electrons and so reduce the number of holes. The nominally divalent impurities Ni and Zn also affect n, although less so, and do so in opposite directions, with

TABLE I. The effect of various impurities on several properties. $\Delta n/n$ is the change of carrier concentration from Ref. 11, p_{eff} is the effective magnetic moment from Ref. 9, x_c is the critical concentration at which T_c goes to zero, and x_{MI} is the concentration at the MI transition.

Impurity	$\Delta n/n$ per at.% (%)	p_{eff} (μ_B)	x_c (at.%)	x_{MI} (at.%)	$\Delta n/n$ at x_{MI} (%)
$Fe^{3+}(3d^5)$	−11.1	4.9	1.8	3.6	−40
$Co^{3+}(3d^6)$	−11.8	1.2	2.65	3.4	−40
$Ni^{2+}(3d^8)$	−4.7	0.7	4.4	4.85	−23
$Zn^{2+}(3d^{10})$	+4.5	1.1	2.85	10.4	+47
$Ga^{3+}(3d^{10})$	−8.4	1.1	2.5	3.45	−29

Zn increasing and Ni decreasing the carrier concentration. This difference in $\Delta n/n$ for the trivalent and the divalent impurities accounts well for the differences in the dependence of the resistivity slope on x, as shown in Fig. 4(b).

Table I also shows p_{eff}, the effective local magnetic moment per impurity atom, from Ref. 9, x_c, the concentration for which T_c goes to zero, x_{MI} from Fig. 9, and $\Delta n/n$ at x_{MI}. For Zn the Hall-effect data of Ref. 11 go only up to 3.7 at.%, and the value at x_{MI} was found by linear extrapolation.

We see from the table that x_c, while it is always smaller than x_{MI}, does not seem to have any obvious relation to x_{MI}. On the other hand it does correlate with p_{eff}, as already noted in Ref. 9.

There is a significant correlation between x_{MI} and $\Delta n/n$, which becomes apparent in Fig. 10, where we show the last column of Table I ($\Delta n/n$ at x_{MI}) as a function of x_{MI}. Each point on this plot represents one impurity species. For example, the point for Zn is at its value of x_{MI} of 10.4 at.%. For this impurity content the carrier concentration is about 47% higher than in pure $La_{1.85}Sr_{0.15}CuO_4$. It is the only point for which $\Delta n/n$ is positive. The other impurities each decrease the carrier

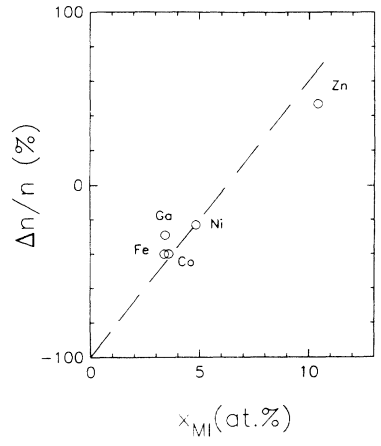

FIG. 10. $\Delta n/n$ at the MI transition as a function of the concentration x_{MI} at which the MI transition takes place.

concentration, with Fe, Co, and Ga having the largest effect, and Ni somewhat less.

The line in Fig. 10 is drawn to guide the eye, with the constraint that it pass through $\Delta n/n = -100\%$ at $x_{MI} = 0$. It represents, roughly and within the uncertainties of this discussion, the interplay of the two factors which we see as superposing to cause the MI transition. First there is the change in carrier concentration, deduced from the Hall-effect data, second the disorder caused by the impurity, which we assume, in this approximation, to be the same for a given value of x, independent of the impurity species.

The line passes through the value $\Delta n/n = 0$ at about $x = 6$ at.%. This point indicates that in the absence of any change in carrier concentration the amount of disorder produced by about 6 at.% of (any) impurity gives rise to a disorder-induced MI transition.

If the carrier concentration is increased, as by the addition of Zn, a larger amount of disorder, i.e., a larger value of x, is required to reach the MI transition. Conversely, a decrease in carrier concentration brings the material closer to the MI transition, which then occurs with a smaller amount of disorder, i.e., with a smaller amount of impurity. Finally, the total absence of carriers, at $\Delta n/n = -100\%$, implies the absence of any metallic character, so that no disorder is required, in addition, to reach the MI transition, and x_{MI} must then be zero.

The line is seen (with all the caution suggested earlier) to represent the superposition of the two factors, the disorder and the change in carrier concentration, which together give rise to the transition from the metallic to the insulating state.

2. *Temperature dependence of the conductivity*

The relation $\sigma = \sigma_0 + m\sqrt{T}$ is in accord with theoretical predictions for disordered metals where the conductivity is determined by electron-electron interactions.[14] It is also in accord with observations on many other systems, including semiconductors and granular metals.[15–19]

In the present case it is followed at low temperatures by all the metallic, nonsuperconducting specimens, but with widely different values of the slope m and up to widely different temperatures T^*. The values of m, σ_0, and T^* are given in Table II for a series of specimens with Fe substitution, and for one specimen from each of the other series, chosen so as to be on the metallic side, but close to the MI transition.

The first important feature evident from the table as well as from Fig. 7 is the sign of the slope m, which is positive for all impurities and for all values of x, no matter how far from the MI transition a given specimen may be. This feature distinguishes the present system from semiconducting materials such as Si:P, Si:B, or Ge:Sb, for which the slope m becomes positive only in the immediate vicinity of the MI transition.[15–17]

The table shows further that the specimens fall into three groups, first Zn and Ni, then Co and Ga, and finally Fe, with progressively decreasing values of m near x_{MI}, and increasing values of T^*. The differences between these groups are illustrated in Fig. 11 where we show the variation of σ with $\sqrt{T}$ for one sample from each group, each with a small value of σ_0. In addition to the large changes between the three groups, the series of six Fe samples shows an increase in T^* and a corresponding decrease in m as σ_0 decreases and the MI transition is approached.

TABLE II. The parameters of the conductivity law, $\sigma = \sigma_0 + m\sqrt{T}$, which holds up to temperature T^*. T_{min} is the temperature of the resistivity minimum.

Sample x (at.%)	σ_0 $[(\Omega\,\mathrm{cm})^{-1}]$	m $[(\Omega\,\mathrm{cm\,K}^{1/2})^{-1}]$	T^* (K)	T_{min} (K)
Zn 10.0	88 ± 10	176	1	
Ni 4.8	12 ± 2	154	1	66 ± 2.5
Co 3.0	130 ± 15	97	2.2	78.5 ± 3.0
Ga 3.4	2 ± 1	84	2.2	94.5 ± 5
Fe 1.5	280 ± 30	100	49	80 ± 2.5
Fe 1.8	230 ± 25	65	55	91 ± 2.5
Fe 2.4	150 ± 15	67	67	100 ± 2.5
Fe 2.7	115 ± 10	56	70	107.5 ± 3.5
Fe 3.0	68 ± 7	50	71	108 ± 3.5
Fe 4.0	0	50	72	128 ± 5

These differences are correlated with the values of T_{min}, the temperature where the resistivity has a minimum as a function of T. The values of T_{min} for some of the specimens are listed in Table II. In Fig. 12 we plot the dependence of T_{min} on the "distance" to the MI transition defined as $(x_{MI} - x)/x_{MI}$. Close to the MI transition, i.e., for $(x_{MI} - x)/x_{MI} < 0.4$, the three groups of impurities, that is Zn and Ni, then Co and Ga, and finally Fe, are seen to have progressively increasing values of T_{min} at the same value of $(x_{MI} - x)/x_{MI}$. For larger values of $(x_{MI} - x)/x_{MI}$ the points for the Zn system do not continue to follow the line for Ni. Instead the points for the Zn system seem to crossover to the group which contains Ga and Co impurities. This peculiarity of the Zn-doped system seems to be an intrinsic property and not

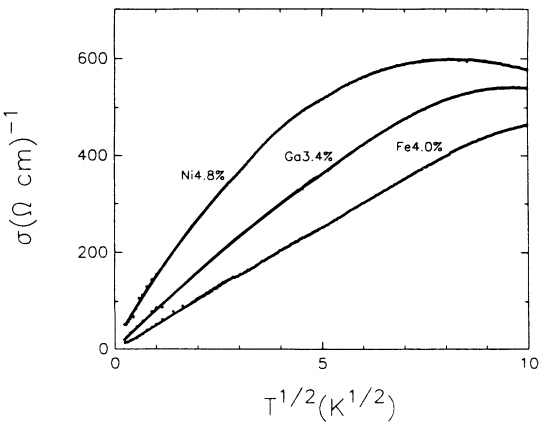

FIG. 11. The conductivity as a function of $\sqrt{T}$ for three samples close to the MI transition.

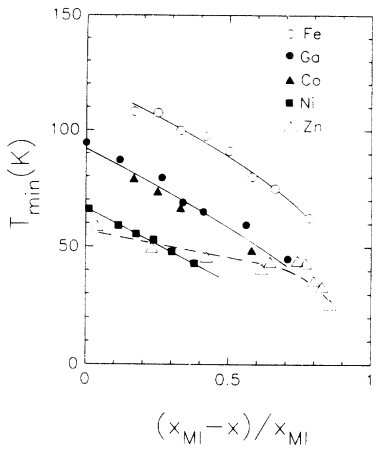

FIG. 12. The variation of $T_{\min}$, the temperature at which the resistivity has a minimum as a function of T, with the distance to the MI transition $(x_{\mathrm{MI}} - x) / x_{\mathrm{MI}}$, for various impurities. The lines are guides to the eye.

related to any structural inhomogeneities of the samples. We have analyzed the x-ray-diffraction patterns for all specimens with Zn and found that the lattice parameters change continuously with the addition of the impurity, indicating that the zinc is indeed incorporated uniformly into the sample.

The temperature $T_{\min}$ represents a crossover temperature below which the electrical transport is dominated by the disorder-induced effects and is therefore a measure of the importance of these effects in the different specimens.

The fact that the three quantities m, T^*, and $T_{\min}$ are closely correlated demonstrates that each of them depends on the strength of the localization and interaction effects. The smallest effect is seen for the divalent impurities Zn and Ni, a larger effect for the trivalent impurities Co and Ga, and the largest effect for Fe. In particular we note that the temperature T^* of about 70 K, up to which the $\sqrt{T}$ dependence is observed in the Fe specimens, is unusually large.

The increase of T^* and the decrease of m and σ_0 with the addition of Fe impurities suggest that these features are the result of the increased spin scattering caused by the presence of the iron. More precisely, we conclude that these features arise from the influence of the spin scattering on the electron-electron interactions. Strong spin scattering is expected to suppress the triplet channel in the particle-hole scattering amplitude, and so to lead to a decrease of σ_0. The positive slope m is then expected even for small impurity contents.[20,21] We know of no other disorder-induced scattering process which would affect the conductivity in this way.

The impurity-induced suppression of σ_0 is similar to the effect of an external magnetic field on the $\sqrt{T}$ dependence of the conductivity in other disordered systems, such as Si:P,[15] Si:B,[17] and granular aluminum.[18] In those cases it is the external magnetic field which is responsible for the suppression of the triplet channel in the particle-hole scattering amplitude.

We can estimate the spin scattering rate in our samples from the value of $T_{\min}$, since for all temperatures below $T_{\min}$ the triplet-channel suppression should be effective, so that at $T_{\min}$, $\hbar/\tau_s \simeq k_B T_{\min}$. For the 4% Fe sample with $T_{\min} \sim 130$ K we find $\tau_s \simeq 6 \times 10^{-14}$ s. For the other Fe samples $T_{\min}$ is somewhat smaller leading to larger values of τ_s.

For other impurities $T_{\min}$ is considerably smaller. In addition, the conductivity is strictly linear versus $\sqrt{T}$ only up to the temperature T^*, with $T^* \ll T_{\min}$ (see Table II). These facts indicate that the spin scattering rate induced by the other impurities is smaller than for Fe, in keeping with the smaller values of the effective magnetic moments (Table I). Nevertheless, the positive values of the slope m indicate that the spin scattering affects the conductivity in these cases also.

The effect of spin scattering may differ between the impurities even when their effective magnetic moments are equal, because of their different effect on the carrier concentration. Since this difference affects the position of the Fermi level with respect to the mobility edge it is also going to affect the electron-electron interactions in the disordered system. In particular, the samples with Zn display much lower $T_{\min}$ than those with Co or Ga at the same value of x, even though their effective magnetic moment is the same. This result is presumably related to the increase of the number of carriers in the Zn system, as compared to the decrease in the Co and Ga systems.

Other effects may also contribute to the differences in the low-T conductivity between the various impurities. These may include, e.g., the inhomogeneous spin localization, as observed in the Si:P system,[22] the formation of impurity-related defects, as proposed by Finkel'stein *et al.* for the Zn-doped (La-Sr)CuO_4 system,[23] and the formation of spin polarons, as observed in some magnetic semiconductors.[19,24] The detailed explanation of the trends which we observe may only be possible after unraveling the microscopic local effect of each impurity.

3. *Critical exponent*

For the two impurity species, Fe and Zn, we can characterize the approach to the MI transition from the metallic side by fitting the data to the expression

$$\sigma_0 = A\,(x_{\mathrm{MI}} - x)^{\nu}. \tag{1}$$

For the Fe system we obtain the parameters $A = 375 \pm 25\ (\Omega\,\mathrm{cm})^{-1}$, $x_{\mathrm{MI}} = 3.6 \pm 0.1$ at.%, and $\nu = 0.92 \pm 0.1$, and for the Zn system $A = 840 \pm 100\ (\Omega\,\mathrm{cm})^{-1}$, $x_{\mathrm{MI}} = 10.4 \pm 0.1$ at.%, and $\nu = 0.7 \pm 0.1$. Figure 13 is a log-log graph of σ_{00} as a function of $(x_{\mathrm{MI}} - x)/x_{\mathrm{MI}}$, together with the best-fitting straight line. Despite the large uncertainities of the parameters there is little doubt that the critical exponent for the Fe system is close to one. This value of the exponent is in accord with the prediction of the scaling theory for the MI transition driven by long-range interactions in the presence of spin-flip scattering.[14,21]

As seen in Fig. 13 the determination of ν for the Zn system relies most heavily on one data point, for 10 at.%, and therefore the value of the critical exponent, $\nu = 0.7$, is less reliable than for the Fe system. We would like to

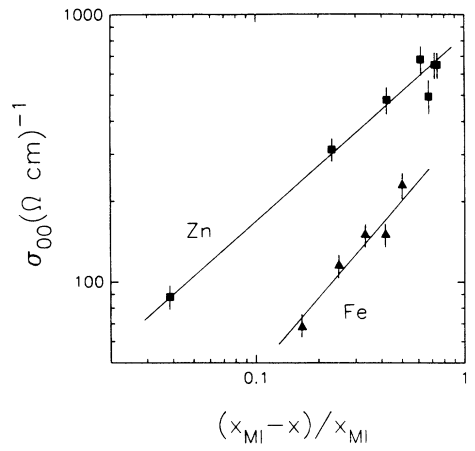

FIG. 13. σ_{00} as a function of $(x_{MI} - x) / x_{MI}$ for Fe and Zn impurities. The slope of the straight lines is equal to 0.92 ± 0.1 and 0.7 ± 0.1 for Fe and Zn, respectively.

point out, however, that the observed reduction of the critical exponent from 1 is not unreasonable. A change of the critical exponent from the value of 0.65 to 1 in the presence of a magnetic field was recently observed for Si:B.[17] It is possible that in the present case the reduction of ν is the result of a smaller spin scattering rate in Zn-doped specimens.

4. *Magnetoresistance*

Depending on the impurity content we observe either a positive or a negative magnetoresistance (MR) [Figs. 8(a)–8(d)]. A positive MR is present only in the samples which are close to the superconducting transition. This is best seen in the Zn-doped system, where the difference between x_c and x_{MI} is largest. On the metallic side of the transition, sufficiently far from the superconducting phase, the MR is negative. We therefore associate the positive MR with superconducting fluctuations. We have been unable to describe the field dependence of MR with the standard fluctuation theories.[25] This is not unreasonable since the transition width in our samples is of the order of 1 K, while the measurements are performed at temperatures near 100 mK.

According to the theory of localization and electron-electron interactions a magnetic field produces several effects.[14] One is the antilocalization from the suppression of the coherent backscattering, which leads to a negative MR. The others, which lead to positive MR, are the suppression of the triplet channel in the electron-hole scattering from Zeeman splitting, and the field-induced change in the electron-electron scattering. We do not observe any positive MR, indicating that the effects related to Zeeman splitting are absent. The reason is presumably that for the Zeeman effect to be effective here, the magnetic-field effect would have to be larger than k_BT and also larger than the effect of the spin scattering, i.e., we would have to have $g\mu_BB > k_BT$ and $g\mu_BB > \hbar\tau_s^{-1}$. For $g\mu_BB/\hbar$ to be larger than 6×10^{-14} s the field would have to be larger than 100 T. Similar conditions apply to the positive MR from electron-electron scattering.

A positive MR is more likely to be observed in samples with small spin scattering and hence with a small value of T_{min}. This may indeed be the origin of the "anomalous behavior" recently described by Jing *et al.*[26] in $Bi_2Sr_2Cu0_6$ crystals. They observed a negative MR changing to positive at a temperature of about 2 K, which is close to their T_{min}. On the other hand, Preyer *et al.*[27] observed negative MR in a $La_{1.98}Sr_{0.02}Cu0_4$ crystal with a large value of T_{min} (~ 100 K).

The negative MR which we observe is probably not the result of the suppression of coherent backscattering since in our case backscattering is already suppressed at zero field by the the large spin scattering. It is more likely to be caused by the suppression of the spin disorder by the magnetic field as in spin glasses.[28] Another example of the suppression of the spin disorder by a magnetic field, leading to a negative MR, has been observed in the magnetic semiconductors $Gd_{3-x}V_xS_4$,[24] $Cd_{1-x}Mn_xSe$, and $Hg_{1-x}Mn_xTe$.[19] In these cases the bound magnetic polarons are centers of spin disorder scattering and the field-induced ordering of the polaron magnetic moments results in the negative MR. It is possible that a similar mechanism exists in the high-T_c oxides as recently proposed by Dietl.[29]

A negative MR implies the possibility of a field-induced transition from the insulating state to the metallic state. Figure 14(a) shows data for the 4 at. % Fe sample, which from all indications is insulating in zero field (see Fig. 9). Extrapolation of the curves of σ against $\sqrt{T}$ leads to zero-temperature values which are negative in a small field (0.5 T) and positive in larger fields. The field dependence is shown in Fig. 14(b). We see that above 1 T the conductivity increases linearly with the field. Similar field-induced insulator-to-metal transitions have also been observed in magnetic semiconductors.[19,24]

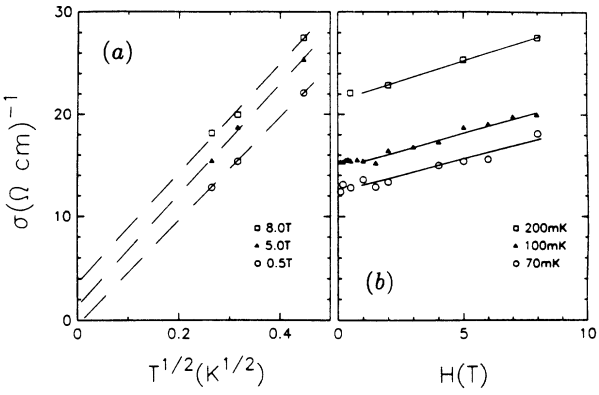

FIG. 14. (a) The conductivity of the 4 at. % Fe sample vs $\sqrt{T}$ in magnetic fields of 0.5, 5, and 8 T. The straight lines extrapolate to $\sigma_0 < 0$ for 0.5 T, and to $\sigma_0 > 0$ for 5 and 8 T. (b) The variation of the conductivity of the 4 at. % Fe sample with field for various temperatures. Above 1 T the data follow straight lines.

5. The destruction of superconductivity

The fact that x_c is smaller than x_{MI}, and apparently uncorrelated with it, leads us to conclude that the MI transition and the disappearance of superconductivity are the result of different factors. The correlation of x_c and p_{eff} suggests, as noted earlier,[9] that the local magnetic moments in the CuO_2 plane are primarily responsible for the destruction of superconductivity. The local magnetic moments also affect the temperature dependence of the conductivity via the influence of the spin scattering on the quantum corrections to the conductivity. The carrier concentration, on the other hand, which has a major effect on $\sigma(T)$, does not seem to have any influence on the superconductivity. These trends are illustrated in Fig. 15 where we show the correlation between p_{eff} and the suppression of superconductivity as measured by $1/x_c$, which is approximately equal to $\Delta T_c/\Delta x$. We also show the correlation between p_{eff} and the value of T_{min} measured at x_c. For all impurities with the exception of Zn the T_{min} dependence mimics that of $1/x_c$. In the case of Zn, as was discussed before, the increase in the carrier concentration weakens the effect of disorder on the conductivity. On the other hand, superconductivity is suppressed with Zn just as fast as with other impurities whose p_{eff} is similar.

Note that the dependence of $1/x_c$ on p_{eff} does not agree with the formula of Abrikosov and Gor'kov for the effect of magnetic impurities on superconductivity,[30] $1/x_c \sim J^2 p_{\mathrm{eff}}^2$, where J is the exchange integral between the free carriers and the impurities. In the present case $1/x_c$ saturates for large p_{eff} instead of increasing with p_{eff}^2. This is not surprising since the interaction between the magnetic moments in the CuO_2 plane must be expected to have a strong effect on the magnetic-moment-induced pair breaking. In addition J may depend on the particular kind of impurity.

Finally we would like to comment on how the relation between superconductivity and the MI transition observed in the the present case compares with others which have been investigated in detail. These include granular aluminum, where magnetic moments and changes in carrier concentration do not play any role, so that there is a pure disorder-induced 3D transition as the grain separation is changed. The experiments show that in this case superconductivity is suppressed by the vicinity of the MI transition, leaving an intermediate metallic but nonsuperconducting range of composition.[31,32] This seems also to be the case in all other 3D systems where the MI transition results from disorder on the atomic scale.[33–35]

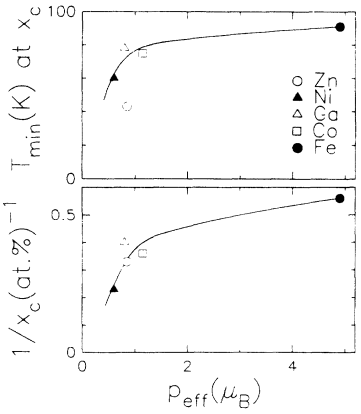

FIG. 15. $1/x_c$ and T_{min} at x_c as a function of p_{eff}. x_c is the concentration where T_c goes to zero, so that $1/x_c$ is approximately proportional to the decrease of T_c with x.

In granular Al-Ge, on the other hand, where the scale of the disorder is of the order of 150–200 Å, an insulator-to-superconductor transition without an intermediate metallic phase is observed.[36,37]

The two-dimensional case is inherently different. Recent experiments on thin films condensed at low temperature show that here superconductivity persists right up to the MI transition.[38,39]

The present study indicates that impurities substituted for Cu in the CuO_2 plane in this and therefore presumably also in other perovskites suppress superconductivity through their local moments before the increasing electron localization near the MI transition can make itself felt. It is possible to introduce disorder by other means than by impurities, but any vacancies or displaced ions will lead to an unbalance in the CuO_2 plane and hence presumably also to local magnetic moments.

B. Insulating side of the MI transition

In this section we discuss the temperature dependence of the resistivity which we observe in the insulating specimens as shown in Figs. 5 and 6.

The relation

$$\rho = \rho_0 \exp(T_0/T)^{1/2}, \tag{2}$$

which is followed by specimens 1–4, has been observed in many disordered insulating systems. The most convincing explanation is that of Shklovskii and Efros[40] in terms of variable-range hopping in the presence of a Coulomb gap.

According to Shklovskii and Efros a Coulomb gap Δ opens up in the density of states at the Fermi level as a result of electron-electron interactions. The parameter T_0 is related to the localization length ξ and the dielectric constant κ by

$$k_B T_0 \simeq \frac{2.8e^2}{4\pi\epsilon_o\ \kappa\xi}. \tag{3}$$

The most probable hopping distance is

$$R = 0.5\xi(T_0/T)^{1/2}, \tag{4}$$

and the corresponding energy is

$$W = k_B T\,\frac{R}{\xi} = 0.5 k_B (T_0 T)^{1/2}. \tag{5}$$

The Coulomb gap can be used to describe the experimental data only when the hopping process is not destroyed by thermal fluctuations, so that for Eq. (2) to be appropriate it is necessary to have $W > k_B T$. On the

other hand, the Coulomb gap will be irrelevant if it is smaller than W, so that we must also have $W < \Delta$.

For hopping energies larger than Δ the electron-electron interactions should have no effect, and we may expect the Mott variable hopping law to be followed,[41] i.e.,

$$\rho = \rho_0 \exp(T_0'/T)^{1/4} \tag{6}$$

with

$$k_B T_0' \simeq \frac{18}{N(E_F)\xi^3}, \tag{7}$$

where $N(E_F)$ is the one-electron density of states at the Fermi energy. For this case the optimum hopping distance is

$$R = 0.4\xi(T_0'/T)^{1/4}. \tag{8}$$

An additional requirement which must be fulfilled in either case is $R > \xi$ so that if the Coulomb gap is to be effective we must have

$$0.5(T_0/T)^{1/2} > 1, \tag{9}$$

and in the Mott case

$$0.4(T_0'/T)^{1/4} > 1. \tag{10}$$

Table III shows the parameter T_0 or T_0' for the relevant hopping process (column 4), and the temperature range for which the process is observed (column 5), for a series of samples. The resistivity of samples 1–4 follows the $T^{-1/2}$ law, while samples 5 and 6 can be described by the $T^{-1/4}$ law below about 1 K.

The values of R/ξ calculated from Eqs. (4) or (8) at the maximum temperature at which the hopping is observed are listed in column 6. It can be seen that the condition $R/\xi > 1$ is fulfilled for samples 1–6. For samples 7–9 this is not the case, indicating that the $T^{-1/4}$ hopping can be expected to be appropriate only for the lower part of the temperature range, i.e., approximately below 0.1 K (if at all). In fact, based on our estimate of x_{MI} from the dependence of σ_{00} on x, sample 8 is just barely insulating whereas sample 9 is barely metallic.

We may now examine the other hopping relations and criteria in order to gain further insight into the approach to the MI transition. For this purpose it would be particularly useful to know the localization length ξ, which diverges at the MI transition. This task is made more complicated by the fact that ξ occurs only in combinations with other parameters whose magnitude and behavior are not well known.

For samples 5–9 Eq. (7) leads to $\xi N^{1/3}$ (column 7). In the absence of other information on the density of states we assume a range of 1–10 states/eV cell as found for $La_{2-x}Sr_{1-x}CuO_4$ from measurements of the heat capacity[42] and susceptibility.[43] The resulting range of values of ξ is listed in the last column of Table III. The large values are consistent with our knowledge that these samples are close to the MI transition. For the more insulating samples 1–4 Eq. (3) leads to the values of $\kappa\xi$ listed in column 8.

We can now estimate the lower limit for Δ from the criterion that it must be at least as large as the optimal hopping energy [from Eq. (5)] at the highest temperature where the $T^{-1/2}$ law is observed. The resulting values of Δ_{min} are shown in column 9.

Additional information on Δ comes from the fact that at the energy $E = \Delta$ the density of states is equal to its value in the absence of electron-electron interactions.[40] It follows that $N(\Delta) = A\Delta^2\kappa^3$, where A is a numerical coefficient.[44] Assuming again that $N \sim 1$–10 states/eV cell we find $\Delta\kappa^{3/2}$ to be in the range 4–12 eV.

The values for Δ_{min} then lead to maximum values for κ, which are shown in column 10. The values are seen to increase rapidly, again consistent with the approach to the MI transition, where κ also diverges.

Finally we may combine κ_{max} with $\kappa\xi$ to get lower limits on ξ for samples 1–4 as shown in the last column of Table III.

In spite of the uncertainties we can now follow the approach to the MI transition quite clearly and consistently. For samples sufficiently far on the insulating side of the transition the Coulomb gap dominates the hopping process and the $T^{-1/2}$ law is observed.

TABLE III. The parameters of the hopping process for a series of samples. μ (column 3) is the hopping exponent and T range (column 5) refers to the temperature range in which the relevant process is observed. The quantities listed in the other columns are defined in the text.

1 Sample No.	2 x (at.%)	3 μ	4 T_0 or T_0' (K)	5 T range (K)	6 R/ξ at T_{max}	7 $\xi N^{1/3}$ ($eV^{-1/3}$)	8 $\kappa\xi$ (Å)	9 Δ_{min} (meV)	10 κ_{max}	11 ξ (Å)
1	Fe 10	$\frac{1}{2}$	260 ± 30	3.5–8	2.85		1800	2	160–340	5–11
2	Ga 10	$\frac{1}{2}$	150 ± 15	1–2.3	4.04		3050	0.8	290–625	5–11
3	Zn 20	$\frac{1}{2}$	23 ± 2.5	0.1–1	2.4		20300	0.21	713–1525	13–29
4	Co 6	$\frac{1}{2}$	9 ± 1	0.1–1	1.5		50210	0.13	1070–2100	24–47
5	Zn12	$\frac{1}{4}$	187 ± 50	0.1–1	1.5 ± 0.1	9.6–11.6				55–142
6	Ni 6	$\frac{1}{4}$	94 ± 30	0.1–1	1.3 ± 0.1	11.9–14.9				68–183
7	Ga 4	$\frac{1}{4}$	3.5 ± 2	0.05–0.25	0.8 ± 0.2	33.3–50.8				190–620
8	Fe 4	$\frac{1}{4}$	0.9 ± 0.7	0.05–0.25	0.6 ± 0.2	50.8–102				290–1250
9	Ga 3.4	$\frac{1}{4}$	2.5 ± 0.2	0.05–0.25	0.7 ± 0.2	35.0–59.5				200–730

As the MI transition is approached the Coulomb interaction becomes screened and the Coulomb gap decreases and eventually disappears. There may now be a region of concentration which is still on the insulating side, but where the hopping process is no longer determined by the Coulomb gap so that Mott variable-range hopping takes over and the $T^{-1/4}$ law is observed.

For the $T^{-1/4}$ law to be observed we must have $R > \xi$. Since R/ξ increases with decreasing T this will occur only at sufficiently low T.

For a given Δ there may also be a transition from $T^{-1/4}$ to $T^{-1/2}$ behavior as a function of temperature depending on whether W is, according to Eq. (5), larger or smaller than Δ. This crossover has been observed by Zhang *et al.*[45] in compensated n-CdSe, although they find a numerical discrepancy between the observed and the expected crossover temperature. Other systems in which a transition from $T^{-1/2}$ to $T^{-1/4}$ has been observed are granular palladium[46] and Ag-Ge films.[47]

Our results are consistent with those of Ellman *et al.*,[48] who observe the two different exponents in two specimens of $La_{2-x}Sr_xCuO_4$, one for $x = 0.02$ for which the $T^{-1/2}$ law is observed, the other for $x = 0.05$, for which the $T^{-1/4}$ law is followed.

Finally we would like to point out that the screening of the Coulomb interaction is not the only possible explanation of the transition from a $T^{-1/2}$ to a $T^{-1/4}$ hopping law. An alternative explanation has been proposed for the case of the magnetic semiconductor $Cd_{1-x}Mn_xSe$,[49] based on the scaling theory of the electron-electron interactions by Finkel'stein.[20] The theory predicts that the single-particle density of states [from Eq. (7)] vanishes at the MI transition as a power law. As a consequence a hopping law with an exponent close to 1/4 may be obtained, with kT_0' different from Eq. (7) in that it is proportional to $\xi^{-3/(\Theta+1)}$, where the exponent Θ depends on the universality class of the MI transition. We have too few samples where we observe the $T^{-1/4}$ law to test this prediction or to establish the value of Θ. Further work will be necessary to study this question.

V. CONCLUSIONS

We have shown that the substitution of other elements for Cu in $La_{1.85}Sr_{0.15}CuO_4$ leads to a metal-insulator transition by the superposition of two factors, namely the change in carrier concentration and the impurity-induced disorder. (See Fig. 10). For each impurity species superconductivity disappears at a concentration x_c, which is smaller than the concentration x_{MI} at the MI transition, leaving a range of concentrations where the specimens are metallic but nonsuperconducting. The critical exponent for the conductivity is close to one for the Fe system and is 0.7 for the Zn system.

Each of the impurities is associated with an effective local magnetic moment whose magnitude is correlated with the supression of superconductivity. The correlation is not, however, that expected from the pair breaking of isolated magnetic moments and indicates, rather, the importance of cooperative magnetic interactions.

In the metallic specimens the conductivity increases as $\sqrt{T}$ at low temperatures. The magnitude of the slope and the temperature to which this variation persists increase strongly with the magnitude of the effective magnetic moment. With iron impurity the $\sqrt{T}$ behavior continues up to the surprisingly large value of 70 K. We conclude that spin scattering plays a major role in determining $\sigma(T)$ through its effect on the quantum corrections to the conductivity. The presence and importance of spin scattering support the indications that this feature is also responsible for the destruction of superconductivity.

All specimens exhibit a negative magnetoresistance (MR) except in the vicinity of the superconducting transition where we see the positive MR associated with the destruction of superconductivity by the magnetic field. We observe a field-induced insulator-to-metal transition in a specimen (4 % Fe) which is just barely on the insulating side of the transition in the absence of a magnetic field. We ascribe the negative MR and the IM transition to the suppression of spin scattering by the magnetic field.

In previous studies the temperature dependence of the resistivity of many kinds of disordered insulators has been shown to be $\rho = \rho_0 \exp(T_0/T)^{\mu}$ with values of μ sometimes identified as 1/2 and sometimes as 1/4. In our specimens both of these values of the exponent occur. By considering the conditions under which a Coulomb gap may be expected to have the dominant influence on the conductivity we have been able to account for the transition from the one to the other of these two exponents in our data, as well as in the data of others. Although other explanations have been put forward from time to time for the exponential behavior of $\rho(T)$, the consistency of the results and the explanations under widely different conditions provides strong confirmation that the description in terms of variable-range hopping in the presence of a Coulomb gap is indeed appropriate.

ACKNOWLEDGMENTS

We would like to thank E. Abrahams, T. Dietl, and A. Ruckenstein for helpful discusions. This work was supported by NSF Grant Nos. DMR 89-17027, DMR 90-24402, and DMR 88-22559 and by a grant from the Polish Committee for Scientific Research.

*Also at Institute of Physics, Polish Academy of Sciences, 02 668 Warsaw, Poland.

[1] J. M. Tarascon, L. H. Greene, P. Barboux, W. R. McKinnon, G. W. Hull, T. P. Orlando, K. A. Delin, S. Foner, and E. J. McNiff, Jr., Phys. Rev. B **36**, 8393 (1987).

[2] T. Hasegawa, K. Kishio, M. Aoki, N. Ooba, K. Kitazawa, K. Fueki, S. Uchida, and S. Tanaka, Jpn. J. Appl. Phys. **26**, L337 (1987).

[3] J. M. Matykiewicz, C. W. Kimball, J. Giapintzakis, A. E. Dwight, M. B. Brodsky, B. D. Dunlap, M. Slaski, and F.

Y. Fradin, Phys. Lett. A **124**, 453 (1987).
[4]W. Kang, H. J. Schultz, D. Jérome, S. S. P. Parkin, J. M. Bassat, and Ph. Odier, Phys. Rev. B **37**, 5132 (1988).
[5]G. Hilscher, Z. Phys. B **72**, 461 (1988).
[6]G. Xiao, A. Bakhshai, M. Z. Cieplak, Z. Tesanović, and C. L. Chien, Phys. Rev. B **39**, 315 (1989).
[7]M. Z. Cieplak, G. Xiao, A. Bakhshai, and C. L. Chien, Phys. Rev. B **39**, 4222 (1989).
[8]H. Tang, G. Xiao, A. Singh, Z. Tesanović, C. L. Chien, and J. C. Walker, J. Appl. Phys. **67**, 4518 (1990).
[9]G. Xiao, M. Z. Cieplak, J. Q. Xiao, and C. L. Chien, Phys. Rev. B **42**, 8752 (1990).
[10]S. Ikegawa, T. Yamashita, T. Sakurai, R. Itti, H. Yamauchi, and S. Tanaka, Phys. Rev. B **43**, 2885 (1991).
[11]G. Xiao *et al.* (unpublished).
[12]M. Z. Cieplak, A. Sienkiewicz, F. Mila, S. Guha, G. Xiao, and C. L. Chien (unpublished).
[13]G. Xiao, J. Q. Xiao, C. L. Chien, and M. Z. Cieplak, Phys. Rev. B **43**, 1245 (1991).
[14]P. A. Lee and T. V. Ramakrishnan, Rev. Mod. Phys. **57**, 287 (1985).
[15]T. F. Rosenbaum, K. Andres, G. A. Thomas, and P. A. Lee, Phys. Rev. Lett. **46**, 568 (1981).
[16]Y. Ootuka, H. Matsuoka, and S. Kobayashi, in *Anderson Localization*, edited by T. Ando and H. Fukuyama (Springer-Verlag, Berlin, 1988).
[17]P. Dai, Y. Zhang, and M. P. Sarachik, Phys. Rev. Lett. **67**, 136 (1991).
[18]T. Chui, P. Lindenfeld, W. L. McLean, and K. Mui, Phys. Rev. Lett. **47**, 1617 (1981).
[19]T. Wojtowicz, T. Dietl, M. Sawicki, W. Plesiewicz, and J. Jaroszyński, Phys. Rev. Lett. **56**, 2419 (1986).
[20]A. M. Finkel'stein, Zh. Eksp. Teor. Fiz. **86**, 367 (1984) [Sov. Phys. JETP **59**, 212 (1984)].
[21]C. Castellani, C. DiCastro, P. A. Lee, and M. Ma, Phys. Rev. B **30**, 527 (1984).
[22]H. Alloul and P. Dellove, Phys. Rev. Lett. **59**, 578 (1987).
[23]A. M. Finkel'stein, V. E. Kataev, E. F. Kukovitskii, and G. B. Teitel'baum, Physica C **168**, 370 (1990).
[24]S. von Molnar, J. Flouquet, F. Holtzberg, and G. Remenyi, Phys. Rev. Lett. **51**, 706 (1983).
[25]S. Hikami and A. I. Larkin, Mod. Phys. Lett. **2**, 693 (1988); A. G. Aronov, S. Hikami, and A. I. Larkin, Phys. Rev. Lett. **62**, 965, 2336(E) (1989).
[26]T. W. Jing, N. P. Ong, T. V. Ramakrishnan, J. M. Tarascon, and K. Remschnig, Phys. Rev. Lett. **67**, 761 (1991).
[27]N. W. Preyer, M. A. Kastner, C. Y. Chen, R. J. Birgeneau, and Y. Hidaka, Phys. Rev. B **44**, 407 (1991).
[28]A. K. Nigam and A. K. Majumdar, Phys. Rev. B **27**, 495 (1983).
[29]T. Dietl (unpublished).
[30]A. A. Abrikosov and L. P. Gor'kov, Zh. Eksp. Teor. Fiz. **39**, 1781 (1961) [Sov. Phys. JETP **12**, 1243 (1961)].
[31]M. Kunchur, P. Lindenfeld, W. L. McLean, and J. S. Brooks, Phys. Rev. Lett. **59**, 1232 (1987).
[32]T. A. Miller, M. Kunchur, Y. Z. Zhang, P. Lindenfeld, and W. L. McLean, Phys. Rev. Lett. **61**, 2717 (1988).
[33]D. J. Bishop, E. G. Spencer, and R. C. Dynes, Solid State Electron. **28**, 73 (1985).
[34]T. Furubayashi, N. Nishida, M. Yamaguchi, K. Morigaki, and H. Ishimoto, Solid State Commun. **55**, 513 (1985).
[35]R. Ludwig and H. Miklitz, Solid State Commun. **50**, 861 (1984).
[36]Y. Shapira and G. Deutscher, Phys. Rev. B **27**, 4463 (1983).
[37]S. Guha and P. Lindenfeld (unpublished).
[38]A. F. Hebard and M. A. Paalanen, Phys. Rev. Lett. **65**, 927 (1990).
[39]Y. Liu, K. A. McGreer, B. Nease, D. B. Haviland, G. Martinez, J. W. Halley, and A. M. Goldman, Phys. Rev. Lett. **67**, 2068 (1991).
[40]B. I. Shklovskii and A. L. Efros, *Electronic Properties of Doped Semiconductors* (Springer-Verlag, Berlin, 1984).
[41]N. F. Mott and E. A. Davis, *Electronic Processes in Non-Crystalline Materials*, 2nd ed. (Oxford University Press, London, 1979).
[42]N. Wada, H. Muro-oka, Y. Nakamura, and K. Kumagai, Physica C **157**, 453 (1989).
[43]R. L. Greene, H. Maletta, T. S. Plaskett, J. G. Bednorz, and K. A. Müller, Solid State Commun. **63**, 379 (1987).
[44]C. J. Adkins, in *Hopping and Related Phenomena*, edited by H. Fritzsche and M. Pollak (World Scientific, Singapore, 1990).
[45]Y. Zhang, P. Dai, M. Levy, and M. P. Sarachik, Phys. Rev. Lett. **64**, 2687 (1990).
[46]S.-L. Weng, S. Moehlecke, M. Strongin, and A. Zangwill, Phys. Rev. Lett. **50**, 1795 (1983).
[47]A. M. Glukov, N. Ya. Fogel, and A. A. Shablo, Fiz. Tverd. Tela (Leningrad) **28**, 1043 (1986) [Sov. Phys. Solid State **28**, 583 (1986)].
[48]B. Ellman, H. M. Jaeger, D. P. Katz, T. F. Rosenbaum, A. S. Cooper, and G. P. Espinosa, Phys. Rev. B **39**, 9012 (1989).
[49]T. Wojtowicz, M. Sawicki, J. Jaroszyński, T. Dietl, and W. Plesiewicz, Physica B **155**, 357 (1989).